ISSN 1063-7826, Semiconductors, 2009, Vol. 43, No. 3, pp. 382–386. © Pleiades Publishing, Ltd., 2009.
Original Russian Text © M.Yu. Morozov, Yu.A. Morozov, V.V. Popov, 2009, published in Fizika i Tekhnika Poluprovodnikov, 2009, Vol. 43, No. 3, pp. 399–404.

PHYSICS OF SEMICONDUCTOR DEVICES

Effect of Pump Wave Reflections on the Excitation of a Dual-Wavelength Vertical-Cavity Surface-Emitting Laser

M. Yu. Morozov, Yu. A. Morozov^, and V. V. Popov

Kotelnikov Institute of Radio Engineering and Electronics, Russian Academy of Sciences (Saratov Branch), Saratov, 410019 Russia

^e-mail: yuri.mor@rambler.ru

Submitted February 21, 2008; accepted for publication May 30, 2008

Abstract—The effect of pump wave reflections on the carrier generation rate and uniformity of carrier population in quantum wells (QWs) of a dual-wavelength vertical-cavity surface-emitting laser has been numerically analyzed. The laser's active region has been described within a mathematical model allowing any number of QWs and arbitrary distribution of carrier generation rate. It is shown that the optimal arrangement of blocking layers in the active region of a dual-wavelength vertical-cavity surface-emitting laser allows one to obtain a very uniform QW population. It is established that pump wave reflections significantly affect the local carrier generation rate and, therefore, the distribution of excited carriers in the laser structure.

PACS numbers: 42.55.Px, 42.60.Fc, 85.35.-p

DOI: 10.1134/S1063782609030233

1. INTRODUCTION

Vertical-external-cavity surface-emitting lasers (VECSELs) are objects of intense study. Under conditions of optical pumping and heat removal from the active region, these lasers emit high-quality radiation with a power up to several tens of watts [1]. In addition, the VECSEL design allows insertion of a nonlinear crystal into a cavity for nonlinear optical frequency conversion. It is known that, due to the resonant increase in the power of the fundamental wave, the intracavity nonlinear optical interaction is much more effective in comparison with the conversion in an external nonlinear crystal [2]. However, until recently, the intracavity second-harmonic generation in VECSELs has been mainly investigated [3, 4]. After the first realization [5] and development of the approach [6] in design of dual-wavelength VECSELs, a possibility arose for effective intracavity generation of combination frequencies [7] and, what is especially important, for difference-frequency generation in the mid- and far-IR regions [8]. Concerning effective semiconductor lasers, these spectral regions are far from being exhausted (actually, only quantum cascade lasers proved their efficiency in these regions). However, at room temperature, the continuous mode is implemented in such lasers only for wavelengths not larger than 10 μm [9]. In this context, detailed study of the characteristics of a laser forming two coaxial beams at two frequencies in a common cavity [5, 6] is of great interest, primarily for nonlinear optical applications.

Note that the problem of designing a dual-wavelength semiconductor VECSEL with lasing wavelengths spaced by $\Delta\lambda = \lambda_L - \lambda_S$ equal to several tens of nanometers is fairly difficult, mainly for the following reasons. First, since the laser's active region must contain at least two sets of different quantum wells (QWs) (shallow and deeper ones for amplifying short-wavelength (λ_S) and long-wavelength (λ_L) radiation, respectively), it is necessary to prevent absorption of short-wavelength radiation in long-wavelength wells. Second, if QWs of different depths can collect optically excited carriers from the same reservoir, almost all carriers are captured to deeper wells. This is due to the shorter carrier capture time and longer carrier escape time, which are characteristic of these wells. The problem of the preferred occupation of deep QWs can be solved using independent pumping of wells of different depths.

To prevent the interaction of optical fields as a result of absorption of λ_S radiation in deep QWs, it was proposed in [5] to locate these wells in electric field nodes of this radiation. In the laser reported in [6], this problem was solved differently: two active regions, composed of wells of different depths, were separated by an optical filter, reflecting short-wavelength radiation and transmitting long-wavelength radiation. For independent optical excitation of shallow and deep QWs, the so-called blocking layers (made of a wide-gap material transparent for laser and pump radiations but impeding carrier transport) were used in [5, 6].

We have numerically simulated the optical excitation of active regions in a dual-wavelength VECSEL [6]. An optical filter in the form of a Bragg mirror, separating the active regions, reflects a large part of the incident pump's wave. As a result, the carrier optical gen-

eration rate in the absorption layers significantly differs from that given by the Lambert–Beer law. Note that only the incident wave, exponentially decaying in the structure's material, is generally taken into account in analysis of coherent optical pumping [10–12].

2. MATHEMATICAL MODEL OF THE VECSEL ACTIVE REGION

The mathematical model of the active region is formulated in the general form and assumes the presence of an arbitrary number of QWs in N sections separated by blocking layers (Fig. 1). As was noted above, blocking layers are assumed to be impermeable for carriers. The ith section contains m QWs of the same type. QWs in different sections may have different composition. A pump wave is incident on the structure from the left and is absorbed by the barrier layers, separating QWs. The model under consideration allows the existence of a reflected pump wave, which interferes with the incident wave. Such reflections, arbitrarily shown in Fig. 1 by bold oppositely directed arrows, always occur in real devices due to the incomplete pump absorption in a single pass through the structure of layers with different refractive indices.

In the absence of a constant electric bias applied to a VECSEL and at charge neutrality, the carrier concentration n in barrier (absorbing) layers obeys the relation [10, 12]

$$D_a\frac{d^2n}{dx^2} - \frac{n}{\tau} + G = 0. \quad (1)$$

Here, D_a is the ambipolar diffusion coefficient and τ is the carrier lifetime in barriers. The local carrier generation rate, due to the pump absorption, is determined as

$$G = -\frac{dS}{dx}\frac{\lambda_p}{hc}, \quad (2)$$

where $S(x)$ is the pump's power density, λ_p is the pump's wavelength, h is Planck's constant, and c is the speed of light. At an exponential decay of pump power (i.e., when the Lambert–Beer law is satisfied), $S(x)$ can be written as

$$S(x) = \frac{P_{in}}{\pi r^2}e^{-ax}, \quad (3)$$

where P_{in} is the pump's power at the input of the absorbing layer, r is the beam's radius, and α is the absorption coefficient. Generally, the power density may differ from the value given by (3) and should be found by solving the wave equation in the laser structure. An example of such a solution will be given below.

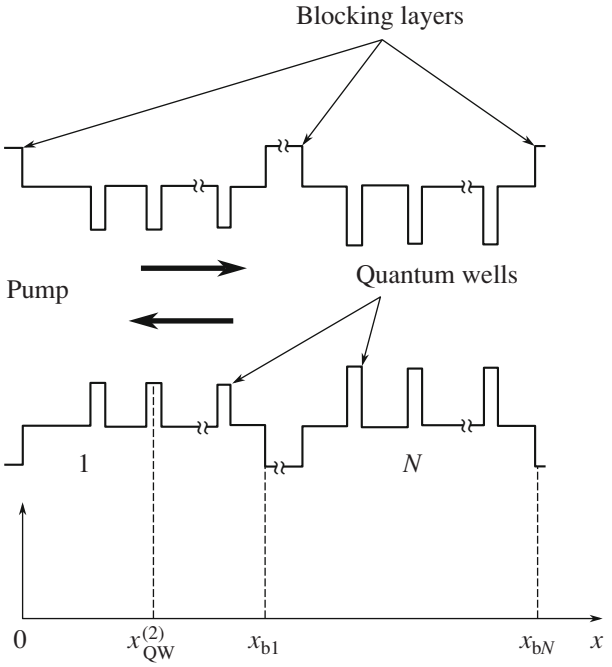

Fig. 1. Energy diagram of the active region model.

Equation (1) allows an exact solution for an arbitrary function G:

$$n(X) = C_1\sinh X + C_2\cosh X + \int_0^X F(\zeta)\sinh(X-\zeta)d\xi, \quad (4)$$

where $X = x/L_a$, $F(X) = -\tau G(L_aX)$, $C_{1,2}$ are constants dependent on the boundary conditions, and $L_a = \sqrt{D_a\tau}$ is the diffusion length. Expression (4) is valid for any point in the barrier layer, i.e., in the homogeneous absorbing layer between two QWs or between a QW and a blocking layer. Since there is a finite carrier flux to a QW from the neighboring barrier layers, all constants $C_{1,2}^j$ are interdependent within each section (j is the barrier layer number in the section). It is assumed that carrier transport through blocking layers is absent; therefore, individual sections are pumped independently. To find the relationship between the constants corresponding to the jth QW, we used the balance equations for carriers at quantum-confinement levels and for those belonging to the continuum in barrier layers at well boundaries:

$$\begin{pmatrix} C_1^{(j+1)} \\ C_2^{(j+1)} \end{pmatrix} = \hat{M}\begin{pmatrix} C_1^{(j)} \\ C_2^{(j)} \end{pmatrix} + \xi\int_0^{X_{QW}^{(j)}} F(\zeta)\sinh(X_{QW}^{(j)}-\zeta)d\zeta\begin{pmatrix} \cosh X_{QW}^{(j)} \\ -\sinh X_{QW}^{(j)} \end{pmatrix}. \quad (5)$$

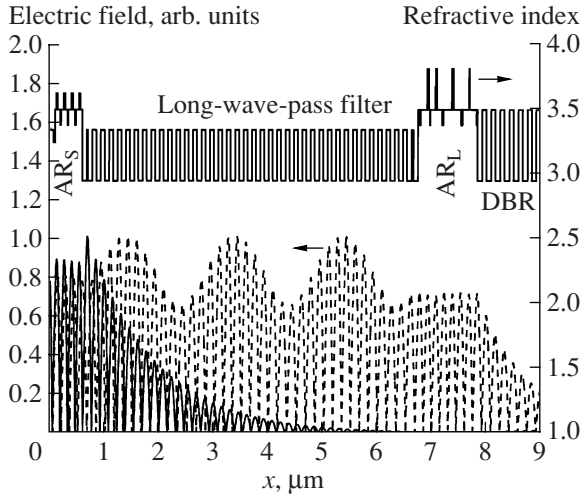

Fig. 2. Refractive index profile (top) and the amplitudes of electric fields with wavelengths (solid line) λ_S and (dashed line) λ_L (bottom).

A more detailed derivation of the last expression, valid for a specific function G (the carrier generation rate determined by the Lambert–Beer law), along with the introduced notation, can be found in [13].

Thus, solution of the problem for determining the carrier's density distribution in barrier layers and QWs is reduced to the determination of $C_{1,2}^{(1)}$. Since there is no carrier flux through the blocking layer at $X = 0$, we obtain

$$\left.\frac{dn}{dX}\right|_0 = C_1^{(1)} = 0. \quad (6)$$

To determine $C_2^{(1)}$, it is necessary to find its value such that, along with the known value $C_1^{(1)}$, would ensure impermeability of the blocking layer at the point X_{b1} (Fig. 1):

$$\left.\frac{dn}{dX}\right|_{X_{b1}} = C_1^{(m_1+1)}\cosh X_{b1} + C_2^{(m_1+1)}\sinh X_{b1} + \int_0^{X_{b1}} F(\zeta)\cosh(X_{b1}-\zeta)d\zeta = 0. \quad (7)$$

Obviously, similar calculations can be performed for other sections, with the origin of coordinates translated to the point corresponding to the blocking layer limiting a given section from the left.

3. ANALYSIS OF THE OPTICAL PUMPING OF A DUAL-WAVELENGTH VECSEL

Let us apply the general model to analysis of coherent optical pumping of a dual-wavelength VECSEL with an optical filter [6]. Figure 2 shows the refractive index profile for the layers forming a laser chip and the distributions of electric field amplitudes at both wavelengths, λ_S (short) and λ_L (long). The structure contains two active regions ($AR_{S,L}$) to ensure generation at two wavelengths, spaced by about 80 nm ($\lambda_S \approx 966$ nm, $\lambda_L \approx 1047$ nm). In accordance with the general scheme in Fig. 1, both active regions (short-wavelength AR_S and long-wavelength AR_L) contain four sections each. Each AR_S section contains two $In_{0.14}Ga_{0.86}As$ wells (QW_S) separated by GaAs barriers. The active region AR_L contains six $In_{0.25}Ga_{0.75}As$ wells (QW_L) in three sections (two in each) and an additional well in the fourth section. The sections of active regions are separated by wide-gap $GaAs_{0.7}P_{0.3}$ blocking layers, which simultaneously play the role of compensators for the compressive strain caused by QW growth. The AR_S region is grown near the structure's surface, while the AR_L region is located in the bulk. The laser's active regions are separated by a long-wave-pass filter composed of alternating quarter-wave AlAs and $Al_{0.3}Ga_{0.7}As$ layers. The filter parameters are chosen so as to reflect short-wavelength radiation and completely transmit long-wavelength radiation through the filter. The distributed Bragg reflector (DBR) grown on the substrate (is not shown in Fig. 1) has a maximum reflection coefficient at λ_L. The position of all QWs approximately coincides with the antinodes of the light electric field at the corresponding wavelength.

Analysis shows that, at specified QW parameters, the growth-induced elastic stress exceeds the critical value. Therefore, additional layers should be introduced into active regions to compensate for this stress. In our case, as was noted above, $GaAs_{0.7}P_{0.3}$ layers play this role. Optimizing the position of blocking layers in the active regions, one can equalize the QW population with carriers. Figure 3 shows the distributions of charge-carrier concentration in barriers and QWs of the AR_S region for (a) blocking layers located at the same distance from the QWs belonging to neighboring sections and (b) optimal arrangement of these layers. The calculations were performed at the laser and pump parameters listed in the table.

The independence of the pumping of individual sections, including dual QWs, manifests itself, in particular, in discontinuities of the plot of the barrier's carrier density at longitudinal coordinates corresponding to the blocking layer positions (Figs. 3a, 3b).

Comparison of the plots in Figs. 3a and 3b and the calculation results show that the optimum arrangement of blocking layers makes it possible to reduce the QW-pumping inhomogeneity approximately from 8% to less than 0.1%. The inhomogeneity factor of QW population was defined as $\chi = \sigma/a_n$, where σ is the standard deviation of the charge density in QWs from their mean a_n. These results were obtained for an *s*-polarized pump beam incident on the structure at an angle of 35°.

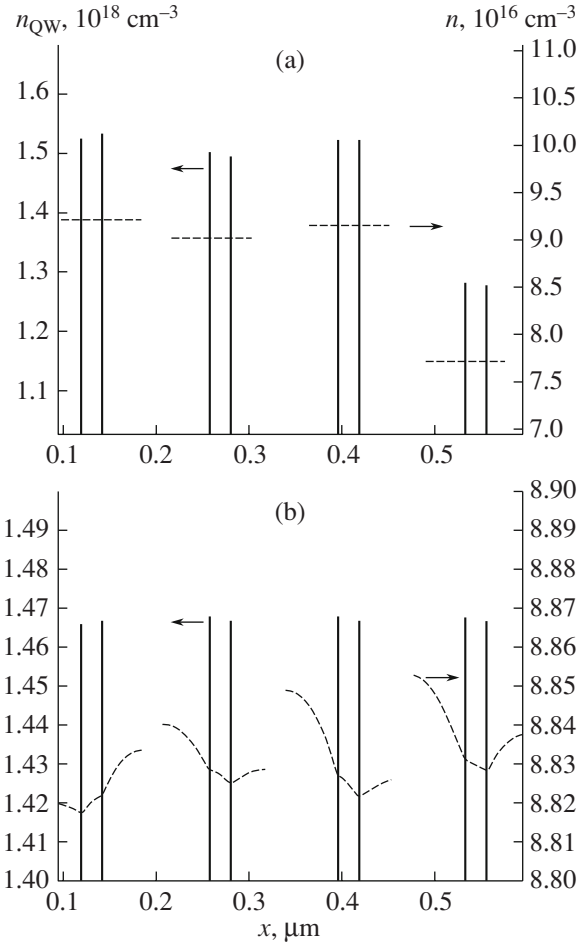

Fig. 3. Distributions of carrier concentrations in (solid lines) QWs and (dashed lines) barriers of the short-wavelength active region AR_S at (a) nonoptimal and (b) optimal arrangements of blocking layers.

The distributions of the carrier's generation rate in the active regions $AR_{S,L}$ for the optimal arrangement of blocking layers are shown in Fig. 4. The G value calculated according to (2) is normalized to the maximum value G_{max} in each region. In the linear absorption mode (unsaturated pumping), the power density $S = 0.5\mathrm{Re}[\mathbf{EH}^*]$ can be found by solving the wave equation for pump radiation in the laser's structure. Here, **E** and **H** are the complex amplitudes of the electric and magnetic pump fields. The wave equation was solved in the geometrical-optics approximation using the transfer-matrix method. Figure 4 shows that the carrier's generation rate significantly differs from the simple dependence

$$G(x) = \frac{P_{in}}{\pi r^2}\frac{\alpha\lambda_p}{hc}e^{-\alpha x},$$

which is valid when only the incident pump wave is present. Pump wave reflections manifest themselves as pulsations of the carrier's generation rate, imposed on

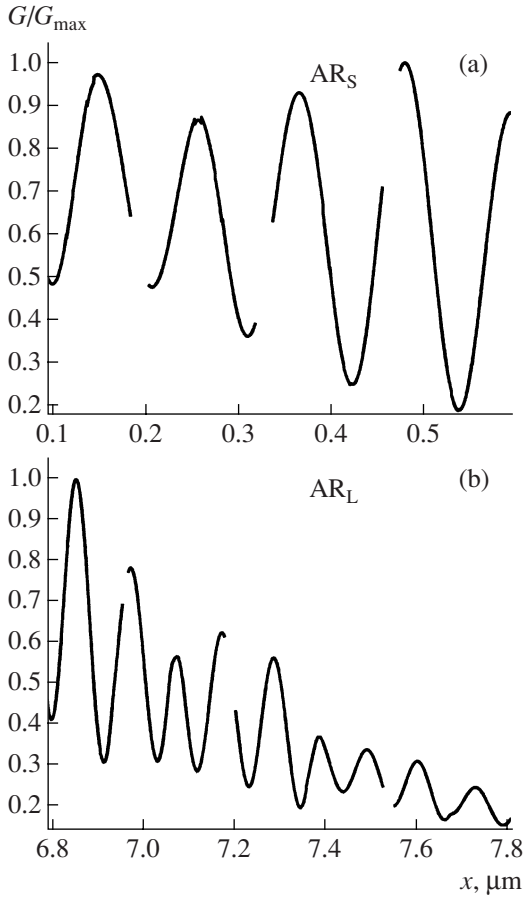

Fig. 4. Carrier generation rate G in the laser active regions (a) AR_S and (b) AR_L, normalized to the maximum value G_{max}.

the exponential decay; note that the pulsation amplitude is comparable (especially in the short-wavelength active region) with the average level of G.

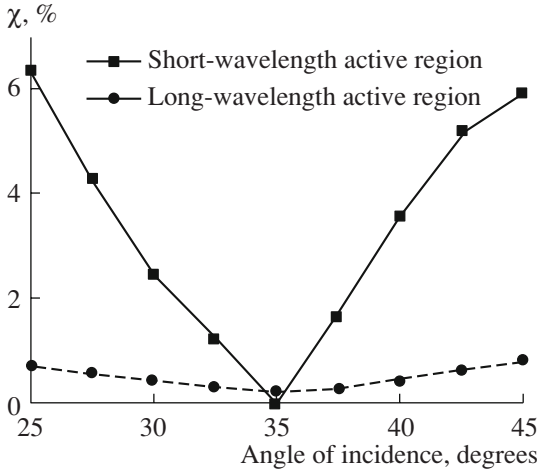

Fig. 5. Dependences of the QW population inhomogeneity in a dual-wavelength VECSEL on the angle of incidence of the pump beam.

Laser and pump parameters

Parameter		Value	Measurement unit
QW_S	τ_c	0.3	ps
	τ_e	5	ps
QW_L	τ_c	0.15	ps
	τ_e	20	ps
t_{QW}		7	nm
τ_r		2	ns
τ		5	ns
D_a		10	$cm^2\ s^{-1}$
α		13200	cm^{-1}
P_{in}		0.2	W
λ_p		808	nm
r		50	μm
λ_S		966	nm
λ_L		1047	nm

Note: τ_c and τ_e are, respectively, the carrier's capture time and the carrier's ejection time from a QW; t_{QW} is the QW thickness; τ and τ_r are, respectively, the carrier lifetimes in barriers and QWs; D_a is the ambipolar diffusion coefficient; α, P_{in}, λ_p, and r are, respectively, the absorption coefficient, input power, wavelength, and spot radius of pump radiation; and λ_S and λ_L are the wavelengths of radiation from QW_S and QW_L, respectively.

The calculated dependences of the inhomogeneity factor χ for the carrier concentration in QWs on the angle of incidence of the pump's beam are shown in Fig. 5. With increasing deviation of the angle of incidence from optimum, χ rapidly increases, especially for the QW population in AR_S. In our opinion, this is another striking demonstration of the role of the pump's wave reflection in excitation of the laser under study. As previously, the calculations were performed for an *s*-polarized pump beam. Qualitatively similar results (omitted here) were obtained for a *p*-polarized pump beam.

4. CONCLUSIONS

A mathematical model of the VECSEL active region has been constructed, which allows an arbitrary number of nonidentical QWs. The latter are located in sections separated by wide-gap layers, which block carrier transport but are transparent for the laser and pump light. These layers can simultaneously compensate for the stress caused by the structure's growth. The model suggests that the local rate of the carrier's optical generation may be an arbitrary function of the longitudinal cavity's coordinates.

The optical excitation of active regions in a dual-wavelength VECSEL [6] has been analyzed. It is shown that optimal arrangement of blocking layers may reduce the QW population inhomogeneity in active regions to a negligible value.

The important role of pump wave reflections in the excitation of active regions of the laser studied is demonstrated. These reflections must be taken into account in simulation of both dual-wavelength VECSELs (similar to those studied in [5, 6]) and conventional single-frequency optically-pumped VECSELs.

REFERENCES

1. A. C. Tropper, H. D. Foreman, A. Carnache, K. G. Wilcox, and S. H. Hoogland, J. Phys. D **37**, R75 (2004).
2. V. G. Dmitriev and L. V. Tarasov, *Applied Nonlinear Optics* (Fizmatlit, Moscow, 2004) [in Russian].
3. G. B. Kim, J.-Y. Kim, J. Lee, J. Yoo, K.-S. Kim, S.-M. Lee, S. Cho, S.-J. Lim, T. Kim, and Y. Park, Appl. Phys. Lett. **89**, 181106 (2006).
4. L. Fan, T.-C. Hsu, M. Fallahi, J. T. Murray, R. Bedford, Y. Kaneda, J. Hader, A. R. Zakharian, J. V. Moloney, S. W. Koch, and W. Stolz, Appl. Phys. Lett. **88**, 251117 (2006).
5. T. Leinonen, Yu. A. Morozov, A. Härkönen, and M. Pessa, IEEE Phot. Techn. Lett. **17**, 2508 (2005).
6. T. Leinonen, S. Ranta, A. Laakso, Yu. Morozov, M. Saarinen, and M. Pessa, Opt. Express **15**, 13451 (2007).
7. A. Härkönen, J. Rautiainen, T. Leinonen, Yu. A. Morozov, L. Orsila, M. Guina, M. Pessa, and O. G. Okhotnikov, IEEE Phot. Techn. Lett. **19**, 1550 (2007).
8. Yu. Morozov, T. Leinonen, M. Pessa, V. Popov, and M. Morozov, in *Proc. of the 15th Int. Symp. Nanostructures: Physics and Technology* (Novosibirsk, Russia, 2007), p. 48.
9. M. Beck, D. Hofstetter, T. Aellen, J. Faist, U. Oesterle, M. Ilegems, E. Gini, and H. Melchior, Science **295**, 301 (2002).
10. J. Geske, K.-G. Gan, Y. Okuno, J. Piprek, and J. Bowers, IEEE J. Quantum Electron. **40**, 1155 (2004).
11. M. Kuznetsov, F. Hakimi, R. Sparague, and A. Mooradian, IEEE J. Select. Topics Quantum Electron. **5**, 561 (1999).
12. Yu. A. Morozov, T. Leinonen, A. Härkönen, and M. Pessa, IEEE J. Quantum Electron. **42**, 1055 (2006).
13. Yu. A. Morozov, I. S. Nefedov, T. Leinonen, and M. Yu. Morozov, Fiz. Tekh. Poluprovodn. **42**, 473 (2008) [Semiconductors **42**, 463 (2008)].

Translated by Yu. Sin'kov